UCRL-17093

University of California

Ernest O. Lawrence Radiation Laboratory

THE DIFFRACTED X-RAY INTENSITY FROM ALTERNATE HCP AND FCC PLATELETS

TWO-WEEK LOAN COPY

This is a Library Circulating Copy which may be borrowed for two weeks. For a personal retention copy, call Tech. Info. Division, Ext. 5545

Berkeley, California

DISCLAIMER

This document was prepared as an account of work sponsored by the United States Government. While this document is believed to contain correct information, neither the United States Government nor any agency thereof, nor the Regents of the University of California, nor any of their employees, makes any warranty, express or implied, or assumes any legal responsibility for the accuracy, completeness, or usefulness of any information, apparatus, product, or process disclosed, or represents that its use would not infringe privately owned rights. Reference herein to any specific commercial product, process, or service by its trade name, trademark, manufacturer, or otherwise, does not necessarily constitute or imply its endorsement, recommendation, or favoring by the United States Government or any agency thereof, or the Regents of the University of California. The views and opinions of authors expressed herein do not necessarily state or reflect those of the United States Government or any agency thereof or the Regents of the University of California.

Submitted to Acta Crystallographica

UCRL-17093
Preprint

UNIVERSITY OF CALIFORNIA
Lawrence Radiation Laboratory
Berkeley, California

AEC Contract No. W.7405-eng-48

THE DIFFRACTED X-RAY INTENSITY FROM ALTERNATE HCP AND FCC PLATELETS

Shelley D. Dahlgren

September 1966

THE DIFFRACTED X-RAY INTENSITY FROM ALTERNATE HCP AND FCC PLATELETS

Shelley D. Dahlgren*

Inorganic Materials Research Division, Lawrence Radiation Laboratory
Department of Metallurgy, College of Engineering
University of California, Berkeley, California

ABSTRACT

A method for calculating the diffracted streak intensity from an alternate HCP-FCC platelet model is introduced. Distributions in the numbers of atomic layers making up the HCP and FCC platelets are considered. The method can thus be used to calculate the diffracted streak intensities from samples with randomly distributed stacking faults.

The method was used to calculate the intensity of streaks found in an oscillation diffraction pattern from a partially transformed Cu-Si sample. Earlier work on Cu-Si alloys revealed an apparent asymmetry of broadened HCP spots in rotation diffraction patterns. The calculated intensity curve accounts for this apparent asymmetry. Contributions to the calculated intensity from pairs of atomic planes where one plane is in one phase and the other plane is in the other phase are significant when the platelets are thin.

* Presently with Battelle Institute, Richland, Washington

I. INTRODUCTION

It was found[1] that both a stacking-fault model and a thin plate model failed to fully explain the streaked x-ray diffraction patterns from partially transformed Cu-4.84 wt.% Si samples. Specimens of this material which had been quenched from 760°C were face-centered-cubic (FCC), and low temperature aging produced thin plates of a metastable hexagonal-close-packed (HCP) phase which were coherent across close-packed planes with the FCC matrix, i.e., $(00.2)_{HCP} \parallel (111)_{FCC}$. The stacking fault model correctly predicted the absence of streaks through h-k = 3n spots, where n is any integer, when streaks were present through h-k = 3n±1 spots, but this theory also predicted that the existing streak intensity maxima should shift in position as the fault probability increased. This latter effect was not observed. On the other hand, a thin crystallite model explained the observed broadening of both FCC and HCP spots but did not explain the absence of streaks through h-k = 3n spots. It was concluded[1] that both stacking fault and particle size broadening were responsible for the streaks through h-k = 3n±1 spots, and that the h-k = 3n spots were always subject to the stacking fault model non-broadening conditions because the thin HCP plates were coherent across close-packed planes with the FCC matrix. It was also concluded that either stacking faults or thin FCC plates which were coherent with thin HCP plates could give rise to the observed streaking through the FCC spots.

Neither the stacking fault nor the thin crystallite theory could be used satisfactorily to calculate the observed intensity variation along the streaks, thus calculations of the diffracted intensity from

an alternate HCP-FCC platelet model were indicated. The intensity equations developed previously[2,3] for the stacking fault case served as a basis for such calculations.

II. INTENSITY CALCULATIONS

Layers of close-packed spheres can be combined in an ABCABC... sequence[4] to form the FCC structure or in an ABABAB... sequence to form the HCP structure. An ABCABAPC sequence indicates a stacking fault in FCC material. Likewise, FCC and HCP structures can be placed together conveniently by changing the stacking of layers from one sequence to the other, i.e., ABCABABA.... The diffracted x-ray intensity from any such stacking distribution of close-packed atomic layers is given by[2,3]

$$I_{hkz} = K\,\psi_{hk}^{2}\left\{\Sigma_M\,(3P_{M^o}-1)\cos 2\pi Mz + \sqrt{3}\,\Sigma_M\,(P_{M^+}-P_{M^-})\sin 2\pi Mz\right\} \quad (1)$$

when h-k = 3n+1 and where K is a constant; ψ_{hk} is the structure factor for a close-packed atomic layer; M is the number of atomic layers between the layer being considered and an arbitrary M = 0 layer; P_{M^o}, P_{M^+}, and P_{M^-} are, respectively, the probability that a layer M layers away from the M = 0 layer, 1) is not displaced (P_{M^o}), 2) is displaced a fixed positive amount in the plane of the layer (P_{M^+}), or 3) is displaced the fixed negative amount in the plane of the layer (P_{M^-}). With the 0^+ - notation, an FCC structure is thus symbolized by $0^+ - 0^+ - \ldots$ and an HCP structure by $0^+0^+0^+\ldots$, 0-0-0-..., or +-+-+-.... Because every layer must be in a 0, +, or - position,

$$P_{M^o} + P_{M^+} + P_{M^-} = 1. \quad (2)$$

ψ_{hk} is zero except when h and k, which are rhombohedral-hexagonal Miller indices, are integers so that Eq. (1) gives the diffracted intensity along

a row of points in the reciprocal lattice where h and k are constant and z is the reciprocal lattice distance along the row.

Equation (1) is for spots with h-k = 3n+1. The spots remaining to be considered are those with h-k = 3n and h-k = 3n-1. The equations[3] involved in the development of Eq. (1) show that h-k = 3n spots are not broadened regardless of the specific distribution of atomic layers being considered. Spots with h-k = 3n need not be considered further because the intensities along streaks are of interest in the present study. The diffracted intensity through spots with h-k = 3n-1 are obtained by multiplying all of the sine terms in Eq. (1) by minus one.[3] The cosine terms in Eq. (1) give a curve which is symmetrical about $z = \frac{1}{2}$, and the sine terms with $z = \frac{1}{2} - a$, where a is an arbitrary fraction, have the same magnitude but the opposite sign to the same terms with $z = \frac{1}{2} + a$, so that changing the sign of the sine terms in Eq. (1) for spots with h-k = 3n-1 amounts to reversing the z coordinate of the curve which is calculated for h-k = 3n+1 spots. In other words, the curve plotted from z = 0 to z = 1 for an h-k = 3n+1 spot series has the same shape as the curve plotted from z = 1 to z = 0 for an h-k = 3n-1 spot series. The curve from z = P to z = P + 1, where P is any integer, is identical to the curve from z = 0 to z = 1 for the same h and k because $\cos 2\pi M(P+z) = \cos 2\pi Mz$ and $\sin 2\pi M(P+z) = \sin 2\pi Mz$. Thus, once Eq. (1) has been used to obtain the curve for I_{hkz} from z = 0 to z = 1 for h-k = 3n+1 spots, the diffracted streak intensity throughout the entire reciprocal lattice is easily established. The relationship of the intensity I_{hkz} and z to the combined HCP-FCC streaked reciprocal lattice is shown in Fig. 1 for the case where $(00.2)_{HCP} \| (111)_{FCC}$ and $(11.0)_{HCP} \| (\bar{2}02)_{FCC}$.

The distribution of close-packed atomic layers for the stacking fault model differs from the distribution for the alternate HCP-FCC platelet model. The probabilities $P_M o$, $P_M +$, and $P_M -$ are therefore different for the two models and these probabilities must be assembled for the platelet model in order to use Eq. (1) for calculating the diffracted intensity. Assume first that all HCP platelets consist of the same number (N_H) of close-packed atomic layers, i.e., $N_H = C_1$, and that all FCC platelets also possess a constant number (N_F) of atomic layers, i.e., $N_F = C_2$, where C_1 and C_2 are constants. The boundaries between close-packed HCP and FCC phases are not sharp, and it is necessary to define a boundary in order to rigorously establish the values of N_H and N_F for individual platelets. Take the defined boundary as the solid line in Fig. 2 where the upper dashed line is above the last identifiable HCP material and the lower dashed line is below the last identifiable FCC material. The solid boundary line thus is taken intermediate to the two dashed lines. All boundaries encountered in the present work can be defined safely in this way although stacking sequences do exist, e.g., a twin-boundary, for which this definition is not satisfactory. With this definition in mind, the specific probabilities, $P_M o$, $P_M +$ and $P_M -$ can be established for the alternate platelet model.

It is a certainty that any atomic layer in the alternate platelet model is not displaced from itself. Therefore, when $M = 0$, $P_M o = 1$ and $P_M + = P_M - = 0$. Adjacent layers must be displaced relative to each other to be close-packed so that when $M = 1$, $P_M o = 0$ and $P_M + + P_M - = 1$. The relative weights given to $P_M +$ and $P_M -$ can be evaluated by considering whether the $M = 0$ layer was chosen in an HCP platelet or an FCC platelet. The probability that it was chosen in HCP material is $\frac{N_H}{N_H+N_F}$. However, an HCP platelet can have a 0-0-0-... or a 0+0+0+... sequence of layers, and both are equally likely. The probability that the zero layer was

chosen in HCP material with 0-0-0-... stacking is thus

$$ {}^{1}P_{1} = \frac{1}{2} \frac{N_H}{N_H+N_F} . \tag{3} $$

The 0-0-0-... stacking sequence is designated by the heavy black line and the title, route 1, in the chart of Fig. 3. The superscript in ${}^{1}P_{1}$ gives the route number of interest and the subscript designates the specific value of M under consideration. The probability of following the $0^+0^+0^+$... stacking sequence, or route 2 in Fig. 3, is

$$ {}^{2}P_{1} = \frac{1}{2} \frac{N_H}{N_H+N_F} . \tag{4} $$

Similarly, the probability that the M = 0 layer was taken in FCC material (or that route 3 is followed in Fig. 3) is

$$ {}^{3}P_{1} = \frac{N_F}{N_H+N_F} . \tag{5} $$

Only the $0^+ - 0^+ - \ldots$ sequence of planes is allowed for FCC material because the FCC crystal started with is fixed in orientation and transforms to the HCP structure, not to the twinned FCC structure. These are the only choices for first near neighbors so that when M = 1, P_{M^+} equals the sum of the probabilities for following routes 2 and 3 and P_{M^-} is given by the probability for following route 1.

If the M = 0 plane was taken in HCP material with 0-0-0-... stacking, route 1 will be followed with increasing M until a phase boundary is reached, and then an FCC sequence will be followed. No change from route 1 is possible when M = 2 because the twinned orientation FCC structure would result. A consequence of not allowing the twin orientation is that N_H must always be an even number. When M = 3, it is possible to form the

proper FCC structure. The likelihood that it will form depends on where the M = 0 layer was picked in the HCP structure. There are $\frac{1}{2} N_H$ possible choices of the M = 0 layer, where the $\frac{1}{2}$ appears because only half of the total number of HCP planes that could be picked lead to the proper FCC structure. The other half lead to the non-allowed twin FCC structure. To get the total probability that the FCC structure is going to be formed from the 0-0-0-... HCP structure when M = 3, the probability that route 1 is followed through M = 2 is multiplied by the probability that the M = 0 layer was selected as the second atomic layer from the boundary in the HCP phase. This latter probability is $\frac{2}{N_H}$. Thus, the total probability of going over to the FCC structure when M = 3, i.e., of following route 1a in Fig. 3, is

$$ {}^{1}P_a = \frac{2}{N_H} \left(\frac{1}{2} \frac{N_H}{N_H+N_F} \right) = \frac{1}{N_H+N_F} \qquad (6) $$

where the superscript in ${}^{1}P_a$ gives the route number and the subscript designates the offshoot to the route. The specific probability of remaining in HCP material when M = 3 is $1 - \frac{2}{N_H}$ so that the total probability of staying on route 1 when M = 3 is,

$$ {}^{1}P_3 = \left(1 - \frac{2}{N_H}\right) \left(\frac{1}{2}\right) \left(\frac{N_H}{N_H+N_F}\right) = \frac{1}{2} \frac{N_H-2}{N_H+N_F} \ . \qquad (7) $$

No change in structure occurs when M = 4 but when M = 5 a change is possible. The probability of change is the probability that the M = 0 layer was picked four layers from the boundary out of the remaining (N_H-2) layers, and this probability is $\frac{2}{(N_H-2)}$. Thus the total probability of following route 1b when M = 5 is $\frac{2}{N_H-2} \left(\frac{1}{2}\right) \frac{N_H-2}{N_H+N_F} = \frac{1}{N_H+N_F}$, or the same probability as found for following route 1a. Similar conditions arise when M = 7, 9, 11, etc., and a regular pattern of terms appear along route 1 and routes 1a, 1b, 1c ... etc, as shown in Fig. 3.

The total probability that route 1 (Fig. 3) is followed is given by the general term

$$^{1}P_M = \frac{1}{2}\left\{\frac{N_H - (M-1)}{N_H+N_F}\right\} \tag{8}$$

where a new probability appears at every second value of M, i.e., only when M is odd. The probability of following any one of the offshoot FCC sequences, 1a, 1b, 1c, ..., is always $\frac{1}{N_H+N_F}$.

Similar reasoning yields the total probabilities for following route 2, Fig. 3, except that the general term for this case is

$$^{2}P_M = \frac{1}{2}\left\{\frac{N_H - (M-2)}{N_H+N_F}\right\}, \tag{9}$$

and the probability changes only when M is even. The probability for following any one of the offshoot sequences 2a, 2b, 2c, ..., is again $\frac{1}{N_H+N_F}$.

Route 3 is slightly different in that a change of structure can occur for any value of M because all combinations of HCP stacking are allowed. The general term for route 3 is

$$^{3}P_M = \frac{N_F - (M-2)}{N_H+N_F}, \tag{10}$$

and the probability changes with each new value of M. The probability for change to any one of the offshoots from route 3 is $\frac{1}{N_F-(M-3)}$. The total probability of following any one of the offshoots 3a, 3b, 3c, ..., is given by the product of the probability for change times the probability of following route 3 up to this change, thus $^{3}P_{a,b,c\cdots} = \frac{1}{N_H+N_F}$.

The process of evaluating P_{M^o}, P_{M^+} and P_{M^-} becomes one of determining the probabilities along the three routes and their offshoots, then

separately adding together those that lead to 0's, + 's, and - 's for each M. This process is continued until M is equal to or greater than the larger of N_H and N_F. Unless both N_H and N_F are very small (< 10), the probabilities P_{M0}, P_{M+}, and P_{M-} will all be near to one-third when M becomes greater than the larger of N_H and N_F. Equation (1) shows that there is little intensity contribution when the probabilities P_{M0}, P_{M+} and P_{M-} are all near one-third. Thus consideration of probabilities for M greater than the larger of N_H and N_F leads to little change in the calculated intensity.

It is evident that the probabilities for following routes 1, 2, and 3 become zero when $M = N_H + 1$, $M = N_H + 2$, and $M = N_F + 2$, respectively. Thus these routes cease to exist for M's larger than those designated above, and the general terms no longer give the correct probabilities. This does not create a great problem when N_H and N_F are constant, but when distributions in N_H and N_F are considered, the general terms must be corrected to avoid adding negative probabilities. The following discussion deals with the effects of such distributions in platelet sizes.

It was assumed in the above discussion, that both N_H and N_F were constant. This is not likely to be true for systems encountered in practice, and distributions in the numbers of atomic planes making up each phase must be considered. If the probability that an HCP platelet consists of exactly N_H atomic layers is P_{NH}, then the probability of randomly picking an M = 0 atomic layer in an HCP platelet consisting specifically of N_H layers is

$$\frac{P_{NH}N_H}{\sum_{N_H=0}^{\infty} P_{NH}N_H + \sum_{N_F=0}^{\infty} P_{NF}N_F} = \frac{P_{NH}N_H}{\bar{N}_H+\bar{N}_F} . \qquad (11)$$

Here P_{NF} is the probability that an FCC platelet consists specifically of N_F atomic layers, and $\bar{N}_H$ and $\bar{N}_F$ are the average number of atomic layers making up HCP and FCC platelets, respectively. The probability that the M = 0 layer is picked in an HCP platelet with exactly N_H atomic layers and with 0-0-0-... stacking is thus

$$ {}^1p_1 = \frac{1}{2} \frac{P_{NH} N_H}{\bar{N}_H + \bar{N}_F} . \tag{12} $$

The specific probability for a change to FCC stacking when M = 3 is the same as before, i.e., $\frac{2}{N_H}$, thus the overall probability for following the first FCC offshoot (identical to following route 1a in Fig. 3) is

$$ {}^1p_a = \frac{2}{N_H} \left(\frac{1}{2}\right) \frac{P_{NH} N_H}{\bar{N}_H + \bar{N}_F} = \frac{P_{NH}}{\bar{N}_H + \bar{N}_H} . \tag{13} $$

Similarly, the probability for continuing in HCP material with the above stacking when M = 3 is

$$ {}^1p_3 = \left(1 - \frac{2}{N_H}\right) \frac{1}{2} \frac{P_{NH} N_H}{\bar{N}_H + \bar{N}_F} = \frac{1}{2} \frac{P_{NH}(N_H - 2)}{\bar{N}_H + \bar{N}_F} . \tag{14} $$

A chart similar to the one in Fig. 3 can be constructed as before for all M's; however, a separate chart is needed for each specific N_H if the above procedure is followed. Because these charts have the same 0, +, and - sequences, the individual probabilities can be summed and placed on one chart. Thus, when M = 1, the total probability for being on route 1 is

$$ {}^1P_1 = \frac{1}{2} \frac{\sum_{N_H=0}^{\infty} P_{NH} N_H}{\bar{N}_H + \bar{N}_F} = \frac{1}{2} \frac{\bar{N}_H}{\bar{N}_H + \bar{N}_F} . \tag{15} $$

Likewise, when M = 2 or more, each of the probabilities can be summed through use of a general term. As stated previously, however, the general

term will include unwanted negative terms when $M > N_H + 1$. Therefore these negative terms are subtracted, and the general term for following route 1 becomes

$$ {}^1P_M = \frac{\left\{ \sum_{N_H=0}^{\infty} P_{NH} [N_H - (M-1)] - \sum_{N_H=0}^{M-1} P_{NH}[N_H - (M-1)] \right\}}{2(\bar{N}_H + \bar{N}_F)} . \tag{16} $$

It is apparent that

$$ \sum_{N_H=0}^{\infty} P_{NH}[N_H - (M-1)] = \bar{N}_H - (M-1). \tag{17} $$

In summing the offshoot branches, it must be recognized that no new offshoots are formed when $m - 1 > N_H$. When $M = 3$, each platelet size will contribute an offshoot, and the total overall probability that the first offshoot will occur is

$$ {}^1P_a = \frac{\sum_{N_H=2}^{\infty} P_{NH}}{\bar{N}_H + \bar{N}_F} = \frac{1}{\bar{N}_H + \bar{N}_F} . \tag{18} $$

All but the platelets with $N_{H=2}$ will contribute an offshoot when $M = 5$, thus the total probability for this offshoot is

$$ {}^1P_b = \frac{\sum_{N_H=4}^{\infty} P_{NH}}{\bar{N}_H + \bar{N}_F} = \frac{1 - \sum_{N_H=0}^{N_{H=2}} P_{NH}}{\bar{N}_H + \bar{N}_F} . \tag{19} $$

Consequently the general term for offshoots of route 1 is

$$ {}^{1}P_{a,b,c\ldots} = \frac{\sum_{N_H=M-1}^{\infty} P_{NH}}{\bar{N}_H + \bar{N}_F} = \frac{1 - \sum_{N_H=0}^{M-3} P_{NH}}{\bar{N}_H + \bar{N}_F}. \qquad (20) $$

The value of M used in Eq. (20) is the lowest M in the offshoot of interest, e.g., for ${}^{1}P_b$, M = 5. The general term for following route 1 in a chart equivalent to the one in Fig. 3 is given by Eq. (16) and the general term for each of the offshoots of route 1 is given by Eq. (20). Similar equations can be derived by the same method for routes 2 and 3. The general term for route 2 is

$$ {}^{2}P_M = \frac{\sum_{N_H=0}^{\infty} P_{NH}[N_H - (M-2)] - \sum_{N_H=0}^{M-2} P_{NH}[N_H - (M-2)]}{2(\bar{N}_H + \bar{N}_F)}, \qquad (21) $$

and the general term for offshoots of route 2 is

$$ {}^{2}P_{a,b,c,\ldots} = \frac{\sum_{N_H=M-2}^{\infty} P_{NH}}{\bar{N}_H + \bar{N}_F} = \frac{1 - \sum_{N_H=0}^{M-4} P_{NH}}{\bar{N}_H + \bar{N}_F}. \qquad (22) $$

The general term for route 3 is

$$ {}^{3}P_M = \frac{\sum_{N_F=0}^{\infty} P_{NF}[N_F - (M-2)] - \sum_{N_F=0}^{M-2} P_{NF}[N_F - (M-2)]}{\bar{N}_H + \bar{N}_F}, \qquad (23) $$

and the general term for offshoots of route 3 is

$$ {}^{3}P_{a,b,c,\ldots} = \frac{\sum_{N_F=M-2}^{\infty} P_{NF}}{\bar{N}_H + \bar{N}_F} = \frac{1 - \sum_{N_F=0}^{M-3} P_{NF}}{\bar{N}_H + \bar{N}_F}. \qquad (24) $$

One last issue must be considered before the specific probabilities can be assembled for any given set of data. Once an offshoot of any route is started, there is a probability of returning to the original structure which is dependent on the number of atomic layers in the offshoot. The specific probability for this change is equal to the probability that the offshoot phase has the number of atomic planes in it equal to the number of atomic layers in the offshoot. This effect is of secondary importance and can be neglected when N_H and N_F are more likely to be large (> 10) than small. The summing of the 0, +, and - probabilities for each M on all routes and offshoots is accomplished as described previously for the case where N_H and N_F were constant.

III. DISCUSSION

The above development is specifically for an FCC crystal which is in the process of transforming to the HCP phase, although similar schemes can be devised to determine the probabilities for any distribution of close-packed atomic layers. The scheme developed here for the FCC → HCP case will duplicate the analysis for randomly distributed stacking faults[3] if $N_H = 2$ and an appropriate distribution of values is given to N_F. Intensity calculations were limited in the present investigation to the case of interest for a Cu-4.84% Si alloy.

Figure 4 is a portion of a 15° oscillation diffraction pattern from a sample of Cu-4.84% Si which had been quenched from 760°C in water and aged 8 hours at 325°C. (The experimental procedure is given in Ref. 1.) Each of the two major streak and spot series in Fig. 4 is from a different set of hexagonal plates which are parallel to separate FCC octahedral planes. Each of these streaks starts at a 20.0 hexagonal spot (cf. Fig. 1)

and ends near 20.3 HCP. Thus, these streaks pass through h-k = 3n-1 spots.

Estimates of N_H and N_F for the sample discussed above, and a method of dealing with the distributions in N_H and N_F are required before the alternate platelet model can be used to calculate the intensity along the streaks in Fig. 4. The distribution problem will be considered first. If there is a small distribution in platelet sizes around the average, and the average is reasonably large (N_H, $N_F > 10$), then the subtracted terms in Eqs. (16), (21), and (23) will be negligible until M is approximately equal to the number of atomic layers in the average platelet. The total probability for following any of the routes is already small when M is of this magnitude, thus consideration of the subtracted terms has little effect on P_{M^o}, P_{M^+}, and P_{M^-} for the assumed conditions. Neglecting the subtracted terms in Eq. (16), and substituting Eq. (17) into Eq. (16) yields

$$^1P_M \simeq \frac{1}{2} \frac{\bar{N}_H - (M - 1)}{\bar{N}_H + \bar{N}_F} . \tag{25}$$

Equation (25) is very similar to Eq. (8). Likewise Eqs. (9) and (10) approximate the required probabilities for following routes 2 and 3 if N_H and N_F are replaced by their average values in these equations.

The offshoot probabilities [Eqs. (20), (22), and (24)] also do not change greatly until M is large when the distribution in platelet sizes is small, and only a few offshoot probabilities are affected because of the small distribution. Each individual offshoot contributes very little to P_{M^o}, P_{M^+}, and P_{M^-} so that $\frac{1}{\bar{N}_H + \bar{N}_F}$ can be used for all offshoots up to M equal to the average number of atomic layers in the platelet without introducing an appreciable error in the calculated intensity.

Without prior knowledge of the distributions in N_H and N_F, it was assumed that the samples dealt with in the present study had only a small distribution in platelet sizes around average. Thus average values of N_H and N_F were used in Eq. (25) and in Eqs. (9) and (10) for the present calculations. The offshoot probabilities were taken to be $\frac{1}{\bar{N}_H + \bar{N}_F}$. The sample used for the x-ray pattern in Fig. 4 was first estimated from particle size broadening theory to have $\bar{N}_H = 100$ and $\bar{N}_F = 300$. The intensity vs reciprocal lattice distance(z) calculated using these values of $\bar{N}_H$ and $\bar{N}_F$ is given by the dashed line in Fig. 5. It was apparent that these values of $\bar{N}_H$ and $\bar{N}_F$ were too large for a good comparison of the calculated intensity with the streak intensity in Fig. 4. $\bar{N}_H = 10$ and $\bar{N}_F = 30$ were then selected for a second trial and the curve calculated using these values is given by the solid line in Fig. 5. This curve is in much better agreement with the streak intensity in Fig. 4.

The calculated curves show that hexagonal spots with odd ℓ Miller indices have a greater intensity than those with even ℓ indices as shown in the diffraction pattern of Fig. 4. Secondly, both the solid line in Fig. 5 and the diffraction pattern in Fig. 4 show an overlapping of the broadened odd ℓ HCP spots with the FCC spots in their immediate vicinity, giving the appearance of having HCP spots shifted toward FCC spots. The maximum calculated intensity for the 20.1 spot (solid line, Fig. 5) appears at $z = \frac{1}{2}$, but the weighted average intensity for the 20.1 spot definitely is shifted toward the $\bar{2}22$ FCC spot. The eye sees the weighted average and thus HCP spots appear shifted in rotation and oscillation diffraction patterns. A good example of HCP spots appearing shifted toward FCC spots is evident in Fig. 3c through 7d in Ref. 1. A discussion of these spots is found under the sub-title "Apparent Streak Asymmetry" in that paper.

The contribution of terms from the offshoots are due to interactions of atomic planes between phases, and these were summed separately for the case where $\overline{N}_H = 10$ and $\overline{N}_F = 30$. These terms contribute as much as 40% of the intensity to the streaked portion of the pattern and actually subtract some from the main HCP and FCC peak intensities. The intensity contributed by these terms is given by the dotted line in Fig. 5. Attempts to explain the observed intensity variation through thin plate analysis of each phase separately, thus are not justified. The use of two reciprocal lattices, one for each thin phase, does not give the required intensity distribution nor does it explain the absence of streaks through h-k = 3n spots.

ACKNOWLEDGMENT

This work was done under the auspices of the United States Atomic Energy Commission.

REFERENCES

1. Dahlgren, S. D., Flanagan, W. F., and Polonis, D. H., Trans. AIME 236, 1071 (1966).

2. Zachariasen, W. H., Acta Cryst. 1, 277 (1948).

3. Barrett, C. S., Trans. AIME 188, 123 (1959).

4. Read, W. T., Dislocations in Crystals (McGraw-Hill Book Co., New York, 1963) p. 93.

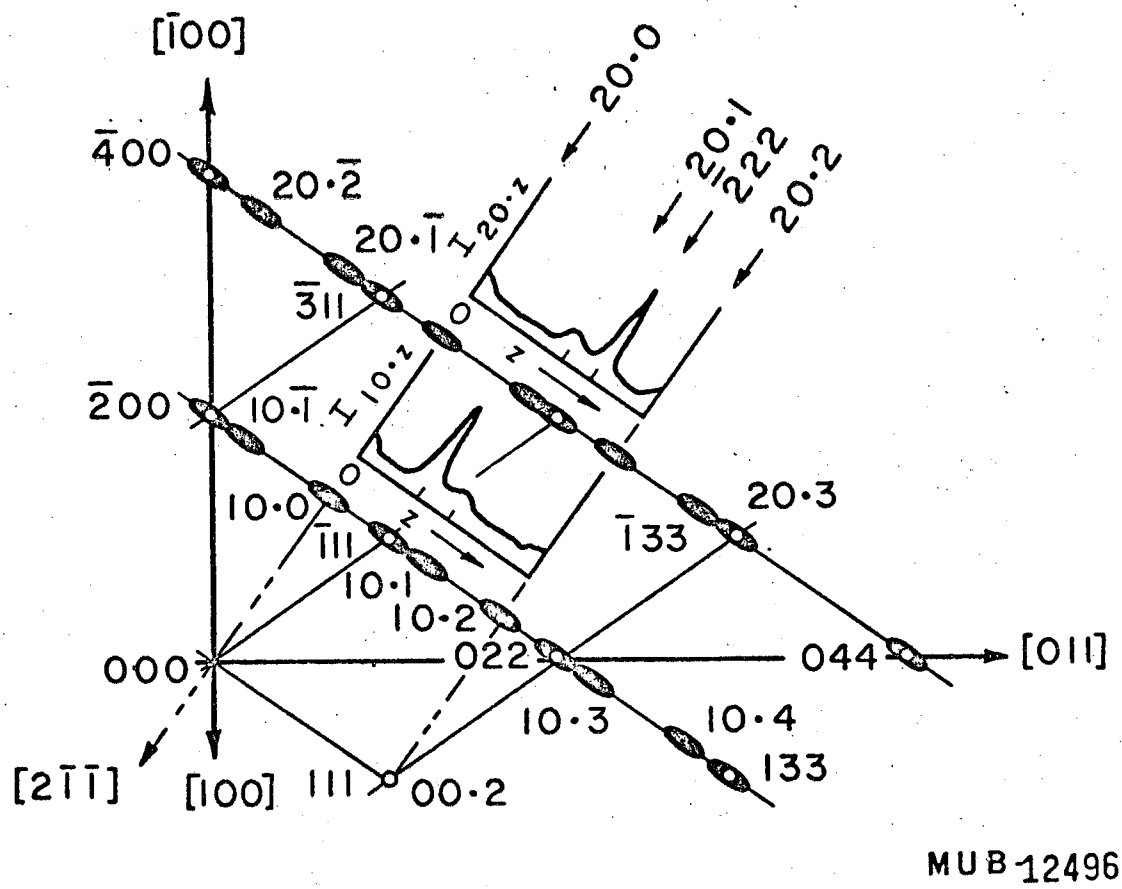

Fig. 1 The combined FCC-HCP reciprocal lattices. The intensity $I_{hk\cdot z}$ vs distance in the reciprocal lattice is shown schematically for h-k = 3n+1 and h-k = 3n-1 spot-streak series. Hexagonal and FCC Miller indices are given by hk·l and hkl, respectively. Small open circles indicate FCC lattice positions.

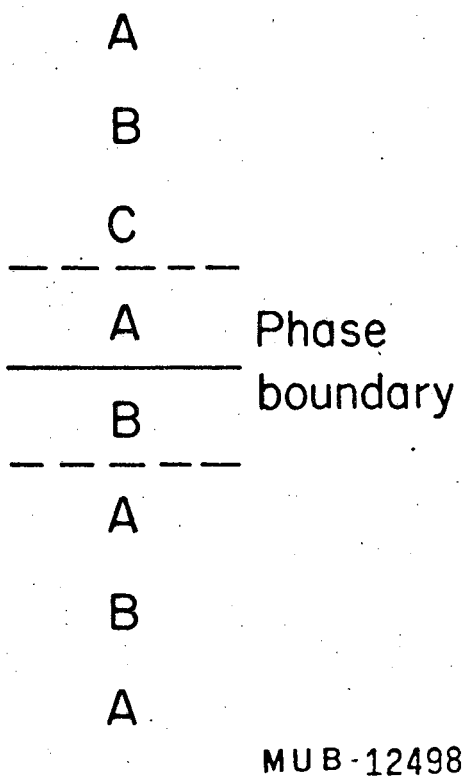

Fig. 2 Diagram to describe the defined phase boundary for the alternate HCP-FCC platelet model.

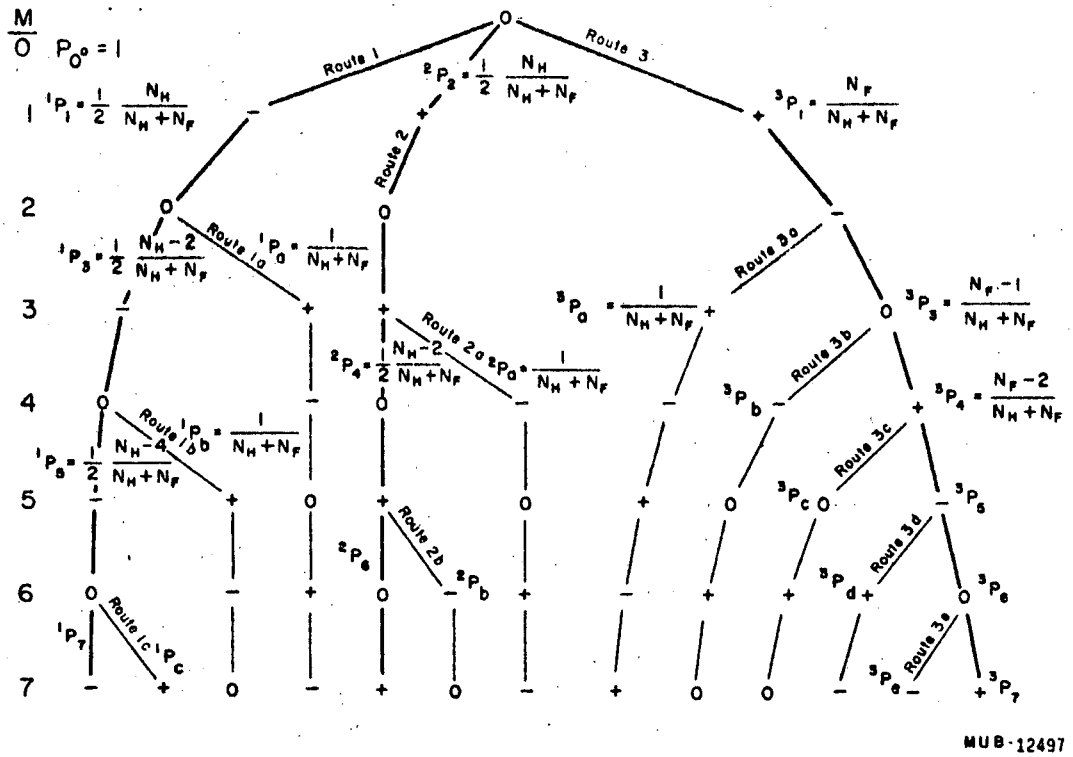

Fig. 3 The total probability for finding atomic layers M layers away from an arbitrary zero layer horizontally displaced 1) no direction, 2) in the plus direction, or 3) in the minus direction from the zero layer. Routes 1 and 2 take into account the spacial relationships for hexagonal stacking of atomic planes, whereas route 3 is for FCC stacking. Offshoot routes 1a,b,c..., 2a,b,c,..., and 3a,b,c,..., account for the spacial relationships of atomic planes in one phase to a zero layer found in the other phase.

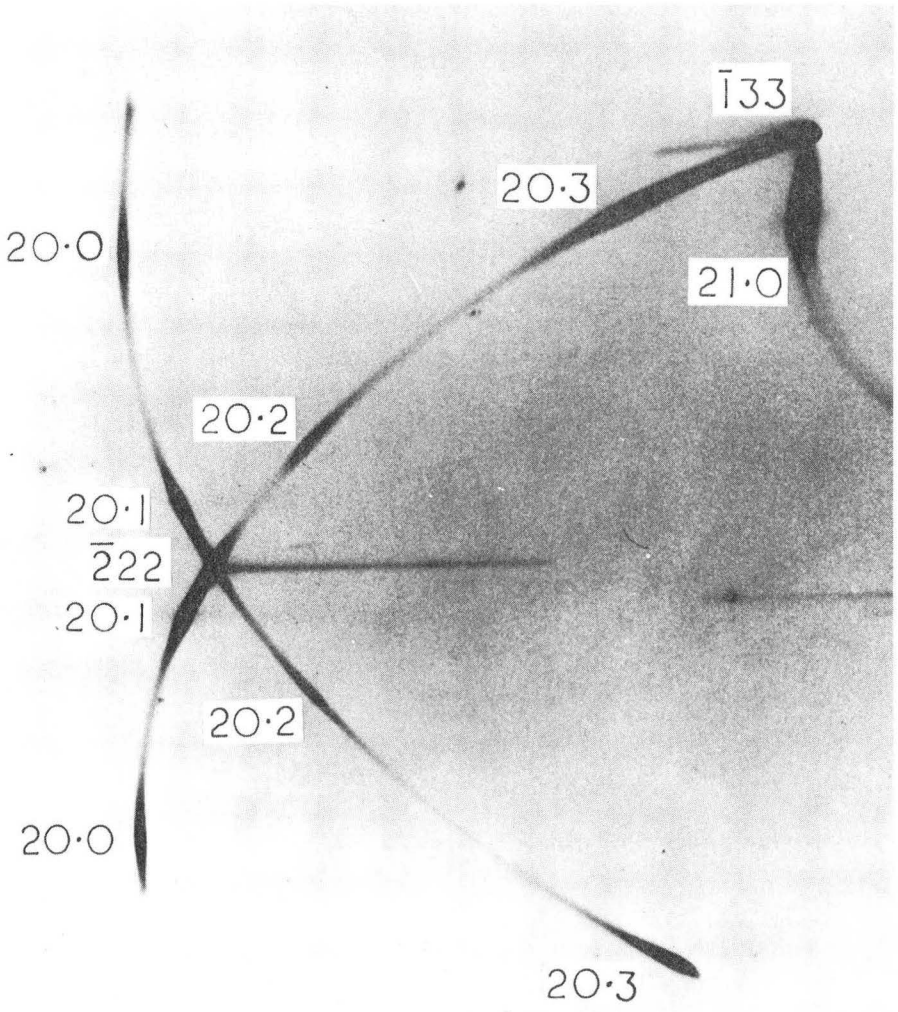

ZN-6005

Fig. 4. A portion of a 15° oscillation diffraction pattern from a Cu-4.84 wt. % Si sample which had been quenched from 760°C and aged 8 hours at 325°C. HCP and FCC spot positions are indicated by Miller indices hk·1 and hkl, respectively.

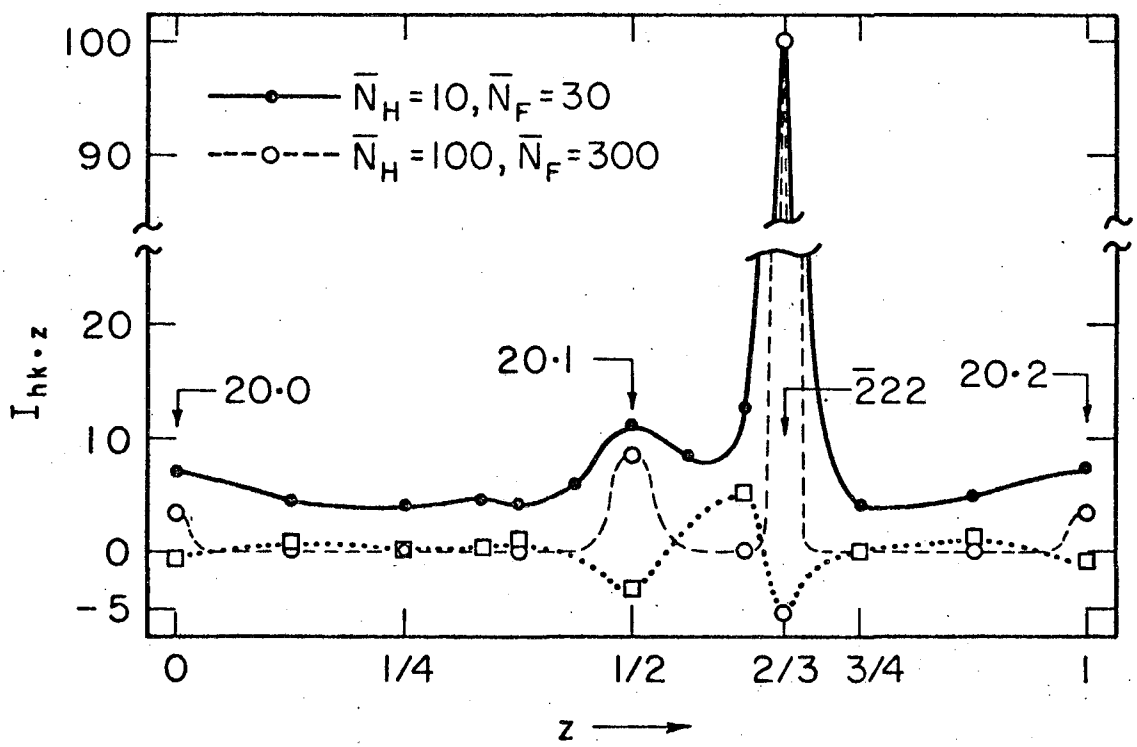

Fig. 5 The calculated intensity vs distance in the reciprocal lattice for $\bar{N}_H = 100$, $\bar{N}_F = 300$ (dashed curve, and $\bar{N}_H = 10$, $\bar{N}_F = 30$ (solid curve). The dotted curve was obtained by summing separately the terms originating from routes 1a,b,c,..., 2a,b,c,..., and 3a,b,c,... . (cf. Fig. 3).

This report was prepared as an account of Government sponsored work. Neither the United States, nor the Commission, nor any person acting on behalf of the Commission:

A. Makes any warranty or representation, expressed or implied, with respect to the accuracy, completeness, or usefulness of the information contained in this report, or that the use of any information, apparatus, method, or process disclosed in this report may not infringe privately owned rights; or

B. Assumes any liabilities with respect to the use of, or for damages resulting from the use of any information, apparatus, method, or process disclosed in this report.

As used in the above, "person acting on behalf of the Commission" includes any employee or contractor of the Commission, or employee of such contractor, to the extent that such employee or contractor of the Commission, or employee of such contractor prepares, disseminates, or provides access to, any information pursuant to his employment or contract with the Commission, or his employment with such contractor.